Cooperativity along kinetic pathways in RNA folding

1996 J. Phys. A: Math. Gen. 29 6265

(http://iopscience.iop.org/0305-4470/29/19/012)

J. Phys. A: Math. Gen. **29** (1996) 6265–6280. Printed in the UK

Cooperativity along kinetic pathways in RNA folding

Gustavo A Appignanesi† and Ariel Fernández†‡

† Instituto de Matemática de Bahía Blanca (INMABB), Universidad Nacional del Sur-CONICET, Av. Alem 1253, 8000 Bahía Blanca, Argentina

‡ The Frick Laboratory, Princeton University, Princeton, NJ 08544, USA

Received 28 November 1995, in final form 5 June 1996

Abstract. Based on kinetic arguments we obtain the time-dependent probability of occurrence of interactions of different ranges for biopolymer folding *in vitro* under realistic time constraints. We focus on random primary sequences in order to fit our results within the context of disordered condensed matter. For the sake of illustration, the results are specialized for RNA folding. They account for the cooperative effects on the different ranges of interaction and quantify the time evolution of their contribution to folding. We also discuss the implications of these results in the understanding of the RNA folding mechanism. Our results furnish evidence supporting the existence of a universal kinetic intermediate in such a process, in accord with previously obtained experimental results.

1. Introduction

The impressive size of conformation space in biopolymer folding rules out the possibility for the biopolymer molecule to find its active conformation by means of an exhaustive random search within biologically relevant renaturation timescales [1, 2]. For RNA folding *in vitro*, the latter are incommensurably shorter than ergodic timescales, as it has been recently pointed out [2]. This fact makes it obvious that biopolymer folding must be carried out through some sort of action-directed pathway. The process must be subject to kinetic control and robust events describable within a coarse description of conformation space must determine the pathways decisively [3, 4].

Since biopolymer folding is a kinetically controlled process, the characterization of the free energy landscape becomes a crucial starting point for any theory which attempts to explain it [3, 5]. In this context, an algorithm to elucidate kinetic folding pathways in RNA based on sequential minimization of the entropy loss has been introduced, showing also its ability as a predictive tool [6]. The applicability of this approach hinges upon the fact that the kinetic barriers for loop closure are best estimated as $-T\,\Delta S_{loop}$, where ΔS_{loop} is the entropic change associated to the reduction in conformational freedom entailed by the formation of the loop. Thus, previous results point to an opportunistic search in the free energy landscape as an expedient to finding the active conformation. By opportunistic we mean that the search follows a 'principle of least effort', that is, the lowest barriers locally dictate the favoured folding step at each stage.

Within this context, the aim of this work is to assess the priority of different ranges of interaction establishing a chronology along dominant folding pathways. Furthermore, we furnish a quantitative measure of the role of cooperativity in the advanced stages of folding, following the initial collapse of the polymer into a universal kinetic intermediate. This

0305-4470/96/196265+16$19.50

intermediate is characterized by single-loop independent interactions of favourable ranges, readily formed starting from a random coil within the milliseconds time frame.

The outline of the paper is as follows. In section 2 we derive the entropic contribution for loop closure in order to determine the activation energy landscape for the folding process. In section 3 we obtain the time dependence of the probability of occurrence of an N-range interaction and quantify the role of cooperative effects in folding. Section 4 displays the results for random chains. In the light of the results shown in section 4, section 5 deals with a proposed picture of the kinetic folding mechanism supporting the existence of a universal kinetic intermediate. Mounting experimental evidence agrees with this picture, as revealed in sections 5 and 6. Section 6 is devoted to justifying the existence of the universal kinetic intermediate by probes which are independent of the previous analysis.

In order to address specific experimental contexts [7], two essential features will be incorporated in future extensions of the theory:

(a) The possibility of forming tertiary motifs such as the pseudoknot (residues in a hairpin engaged in base-pairing with residues outside the hairpin forming an additional stem and loop region [8]).

(b) The role of Mg(II) ions in lowering the kinetic barriers for the occurrence of specific base-pair interactions.

These features are briefly discussed in section 2.

2. Activation barriers in the kinetic control of RNA folding

In general, the observed marginal stability of the folded form of biopolymers [6, 9–13] implies the existence of a force opposing stabilizing chain interactions hitherto ignored: the conformational entropy [14, 15]. The computation of this quantity is tantamount to determining a key feature complementary to the canonical thermodynamic quantities: the activation energy landscape. Specifically, since the process of RNA folding is subject to kinetic control and recent results [6] suggest that folding pathways are governed by a least action principle, we are faced with the necessity of acquiring a precise knowledge of the activation barriers involved in folding events, which implies a quantitative determination of the entropy loss.

The rate-limiting step in RNA loop formation is the process of bringing into close contact the antiparallel regions capable of forming base pairing [16, 17]. As this event implies a loss in conformational entropy, the elucidation of the profile $-T\,\Delta S_{loop}$ (ΔS_{loop} = loss in conformational entropy in the formation of a loop) as a function of loop size becomes a cornerstone in the determination of the activation barriers for folding. Relevant portions of this profile have been obtained elsewhere [18], so we only outline here the physical principles and basic tenets of the previous study.

As is well established, taking into account excluded-volume effects in the closure of a loop of size N in a linear RNA chain, the loss in conformational entropy takes the value [19]

$$\Delta S_{loop} = -\mu R \ln N + K(v) \tag{1}$$

where μ must be taken to be 1.75 for RNA (a polyelectrolite) in a good solvent like water and $K(v)$, which is constant for the different loop sizes, depends on the effective contact volume v. Since this last term is not amenable to an easy direct evaluation, it is obtained by comparing equation (1) with reliable measurements for stable loops.

Equation (1) is valid in the limit of large loops but it cannot be extrapolated for small or moderate-sized loops, since orientational effects for charged moieties (phosphates) are responsible for the breakdown of the logarithmic dependence on N. This is shown as follows.

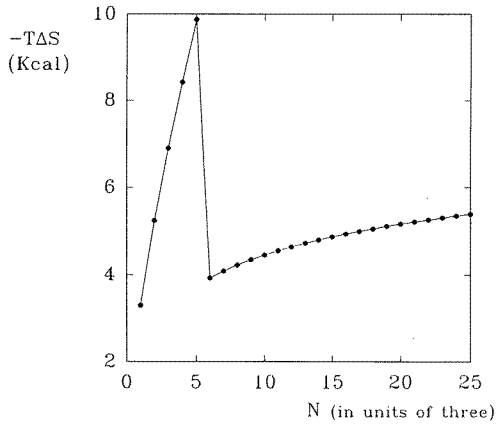

Figure 1. Conformational entropy loop ($-T\Delta S_{loop}$) involved in the closure of a loop of size N. The loop sizes are expressed in units of three (each unit of N represents three nucleotides).

Consider a linear RNA chain immersed in water. The RNA molecule has many internal rotational degrees of freedom. As these rotations are much faster than the folding events we are concerned with, we can average them out whenever we deal with the folding process. This averaging process could be said to be inspired by the Born–Oppenheimer approximation, where comparatively slow nuclear motion is corresponded with folding events and fast electronic motion with backbone rotational freedom. The faster backbone rotations allow for the orientation of the charged phosphate moieties within a specific folding of the chain. This separation in timescales (nanosecond versus millisecond-to-second range) allows us to regard the RNA chain as a rod of fixed circular cross section in the averaging limit. This circular cross section corresponds to twice the mean phosphate–base distance [19]. If we now close a planar loop, we are left with two distinctive domains of the solvent: the inner domain of cluster-like dimensions and the outer bulk-like domain. This points to the existence of a critical loop size beyond which these two domains behave as indistinguishable, being equally capable of solvating the polar phosphate groups of the RNA molecule. But for loop sizes below this critical size, the solvent of the inner domain acquires discrete features and becomes a poorer dielectric. The crucial point here is that the structure of the solvent is *qualitatively* different from the bulk. In this case, the RNA molecule orients its polar groups to the outer domain. This fact causes an extra (orientational) conformational entropy loss which must be reflected in the profile of $-T\Delta S_{loop}$. This contribution of ΔS_{loop} can be evaluated simply by

$$\Delta S_{orient} = R \ln \left[\frac{\Omega_{loop}}{\Omega_{RC}} \right] = R \ln \left[\frac{2^{M-N}}{2^M} \right] = R \ln 2^{-N} = -RN \ln 2 \qquad (2)$$

where Ω is the number of conformations or microscopic realizations of a given topology (Ω_{loop} for a loop of size N within a chain of length N and Ω_{RC} for a random coil of length M). For loops of length less or equal the critical size, this term needs to be considered and becomes the dominant term since it is linear in N, in contrast to the logarithmic dependence on N of the term based on excluded-volume effects. The critical size N_c was determined, based on the consideration of molecular dimensions and regarding the RNA molecule as a rod, as being $N_c = 17$ [18]. For loops of sizes greater than the critical, there is no orientational term and the excluded-volume effects become the exclusively dominant effects. The profile $-T\Delta S$ versus N is displayed in figure 1.

Although the paramount role of Mg(II) ions for certain RNA folding contexts [7] will

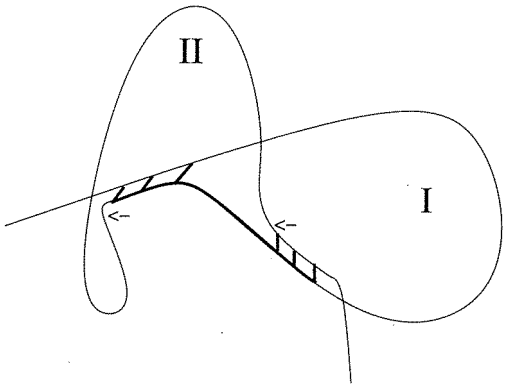

Figure 2. Spatial representation of a pseudoknot comprising hairpin loop I followed by loop II. The region to be oriented concurrently with closure of loop II is displayed by thin curve between the arrows. The thin curve region common to loops I and II is already oriented upon formation of loop I and prevents both loops from being coplanar.

not be explicitly dealt with in this paper, it should be discussed briefly in the light of the orientation arguments presented in this section.

It is known that Mg(II) binds to adjacent phosphates of unpaired nucleotides by forming a coordination complex [20]. Thus, $-T\Delta S_{loop}$ for the process of phosphate orientation concurrent with loop closure is roughly reduced by one half since the 30 kcal mol^{-1} released when a single coordination bond is formed can be actually invested in the orientation of the phosphate adjacent to the one that is already coordinated. This reasoning is corroborated further by the minimal (0.1 kcal mol^{-1}) difference between the free energy of formation of a bulge loop of size one and one of size two (the size-one loop does not require magnesium while in the size-two loop chelating coordination makes both phosphates behave as a single entity).

Throughout the following sections we shall only be concerned with planar secondary interactions forming Watson–Crick (C–G, A–U; C = cytosine, G = guanosine, A = adenine, U = uracil) base pairs. Further research will deal with certain tertiary structure motifs as well. Thus, the activation barrier for pseudoknot formation can be easily obtained from the orientational arguments introduced here: suppose a hairpin I has been formed (see figure 2) and we desire to derive the activation barrier associated with forming loop II, and suppose that loop I and loop II are below the critical range. We first observe that both loops cannot be coplanar since the common region (thick full curve in figure 2) has already been oriented upon formation of loop I and, as such, it is solvated by bulk water, a condition not easily relinquished. Should loop II form coplanarly, it would affect the self-energy of hydration of the phosphates in the thick curve common region by drastically reducing the dielectric in which these phosphates are immersed. Thus, the loops should be formed in the manner suggested by figure 2 and $-T\Delta S_{loop}$ should be equal to $RTL\ln 2$; where L is the number of nucleotides exclusively in loop II in between the arrows, as indicated in figure 2.

3. Probability of occurrence of interactions of range N: time evolution and cooperativity

In following the kinetics of RNA folding, an object which seems worthwhile to focus on is the time evolution of the probability of occurrence of N-range interactions. This function

will provide information on the preeminence of different folding events at different times and will enable us to make detailed inferences on folding pathways.

In order to study the time evolution of N-range interactions in RNA, we model the RNA molecule as a chain of constitutive units or nucleotides, but we are not interested in an atomic resolution, rather in a structure resolved up to the level of the contact topology or base-pairing pattern (BPP). The contacts are generated via the base-pairing of antiparallel regions along the chain following Watson–Crick complementarity. The level of coarsening of the structure description is the one compatible with our data on entropic and enthalpic contributions and fits with fundamental thermodynamic forces and timescales which account for the robustness and expediency of the folding process.

We choose an infinite RNA chain with random primary sequence in order to *deal with entropic effects only*. The *level of detail suffices to manifest the general phenomena* we are interested in, as will be presently discussed.

Since the primary sequence of the chain is random, it would be highly unlikely to find strands with more than three complementary antiparallel nucleotides, so we only consider contacts formed by three base-pairs. Three is the minimal number of base pairs that stabilize a contact entailing the formation of a loop, as well as the size of the smallest stable loop which can be formed. Therefore, we divided the chain into units of three nucleotides. The ranges of interaction and loop sizes are expressed in such units. For the sake of this analysis, only loops of *actual* size $3N$ will be considered.

With the $-T\Delta S$ versus N profile in hand, and having defined the system of interest, we can study the time evolution of the probability of N-range interactions. First, we must consider the time evolution of the probability of occurrence of an interaction of range N in a single independent folding event (involving a simple hairpin loop) starting from an unfolded chain or random coil. An interaction of range N is one which has N constitutive elements in between the antiparallel complementary regions which form the contact. In this case, the formation of an interaction of range N corresponds to the closure of a loop of size N. The probability of occurrence of an N-range interaction is therefore gained with the creation of a loop of size N and is lost with the destruction (unfolding) of such a loop. So, we have

$$\frac{\partial p(N,t)}{\partial t} = v_+(N) - v_-(N)p(N,t) \tag{3}$$

where $v_+(N)$ is the rate of construction of a loop of size N starting from the random coil, $v_-(N)$ is the corresponding rate of destruction and $p(N,t)$ is the probability of occurrence of an interaction of size N at time t from an unfolded chain and by means of a single independent step. The rates of construction and destruction are, respectively [2],

$$\begin{aligned} v_+(N) &= fn\exp(\Delta S(N)/R) \\ v_-(N) &= fn\exp(\Delta H/RT) \end{aligned} \tag{4}$$

where $f \sim 10^6$ is the unimolecular constant for base pairing, $n = 3$ is the number of base pairs needed to stabilize a contact, $\Delta S(N)$ is the loss in conformational entropy associated with the formation of a loop of size N and ΔH is the amount of heat released when forming a contact concurrently with closure of an N-loop. This last quantity is independent of loop size, so $v_-(N)$ is a constant.

From equation (3), the probability of occurrence of an interaction of range N at time t in a single independent event starting from a random coil is

$$p(N,t) = \frac{v_+(N)}{v_-(N)}(1 - \exp(-v_-(N)t)). \tag{5}$$

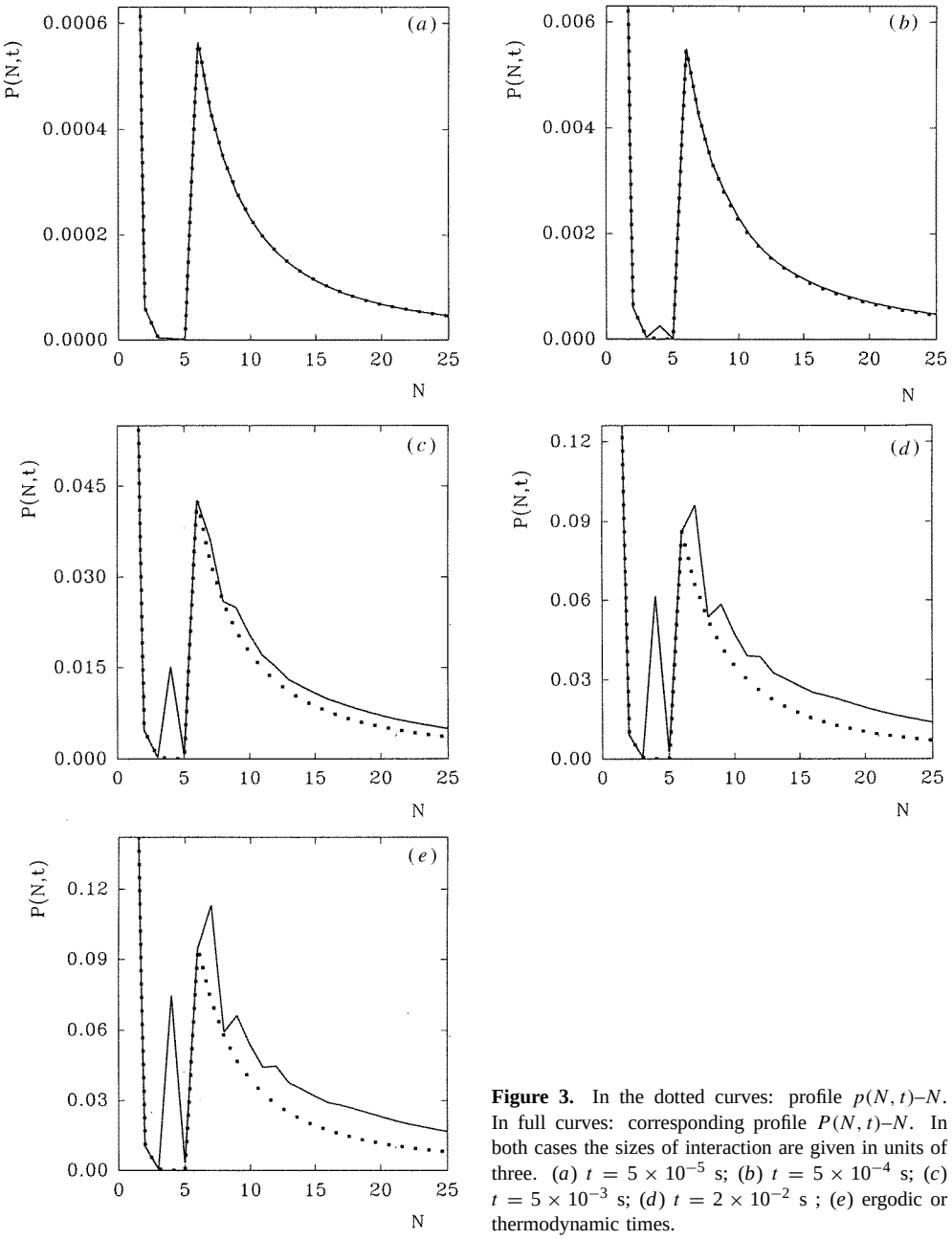

Figure 3. In the dotted curves: profile $p(N,t)$–N. In full curves: corresponding profile $P(N,t)$–N. In both cases the sizes of interaction are given in units of three. (*a*) $t = 5 \times 10^{-5}$ s; (*b*) $t = 5 \times 10^{-4}$ s; (*c*) $t = 5 \times 10^{-3}$ s; (*d*) $t = 2 \times 10^{-2}$ s ; (*e*) ergodic or thermodynamic times.

Note that at $t = 0$ $p(N,t) = 0$ because we are starting from the random coil where there are no interactions established, and that in the thermodynamic limit $p(N,t)$ tends to the Boltzmann distribution law

$$\lim_{t\to\infty} p(N,t) = \frac{v_+(N)}{v_-(N)} = \frac{fn\exp(-T\Delta S/RT)}{fn\exp(\Delta H/RT)} = \exp(-\Delta G(N)/RT). \quad (6)$$

In figure 3 we can see, in the dotted curves, the curves $p(N,t)$ versus N at different times. From them we can learn that short-range and moderately long-range interactions

are the most favourable ones, while long-range interactions and medium-range interactions, those involving the closure of loops of size near and below the critical size, are significantly less probable. In figure 3, we can also see that the shape of the curve does not vary with time. This means that the interactions of different sizes would have the same relative probabilities at any time if the folding process was governed by the profile of $p(N,t)$, that is, if all folding events involved the closure of simple loops, without cooperativity between different folding steps. But in the dynamics of the folding process, some interactions *do influence* other subsequent interactions. For example, a long-range interaction of size N would have a negligible probability of being formed within the biologically relevant timescales if it involved the closure of a big loop of size N. But, if there were a previous (or more than one) interaction of range N' already contained in it, the loop to be closed to produce the interaction of range N would be smaller and could greatly increase the probability of occurrence of such interaction. In other cases, for example, a moderately long-range interaction (with an appreciable $p(N,t)$) could see its probability of occurrence greatly diminished if it contained a previously formed short-ranged interaction which shortened the loop to be closed and made it fall within the region of the critical size. These simple examples show us that cooperative effects cannot be neglected as they can be important in the determination of the folding pathways followed by the biopolymer in the nonergodic regime.

To take into account the cooperative effects we introduce the following:

$P(n,t)$ = Probability of occurrence of an interaction of range N in the time interval $(t, t+\mathrm{d}t)$.

Once we have considered the most probable folding events, this probability can be written in the following way:

$$\begin{aligned}
\frac{\partial P(N,t)}{\partial t} = {} & v_+(N) - Ap(N,t) + \left(\frac{1}{N-3}\right)\sum_{N'=1}^{N-3}(N-N'-1) \\
& \times p(N',t)(v_+(N-N'-2) - Ap(N-N'-2,t)) \\
& + \left(\frac{1}{(N-6)(N-5)}\right)\sum_{N'=1}^{N-6}\sum_{N''=1}^{N-5}(N-N'-N''-2)(N-N'-N''-3) \\
& \times p(N',t)p(N'',t)(v_+(N-N'-N''-4) - Ap(N-N'-N''-4,t)) \\
& + \left\{\frac{1}{N_T-N_c}\sum_{M>N_c}(M-N-1)p(M,t)\right. \\
& \times (v_+(N;M-N-2) - Ap(N;M-N-2,t)) \\
& + \frac{1}{N_c-N-2}\sum_{(N+3)\leqslant M\leqslant N_c}(M-N-1)p(M,t) \\
& \left.\times (fn - Ap(N;M-N-2,t))\right\} \\
& + \left(\frac{1}{(N_T-N-6)(N_T-2N-11)}\right)\sum_{M\geqslant N+7}\sum_{N'=1}^{M-N-5}(M-N-N'-2) \\
& \times (M-N-N'-3)p(M,t)p(M;M-N'-2,t) \\
& \times (v_+(N;M-N'-N-4) - Ap(N;M-N'-N-4,t)) + \cdots
\end{aligned} \tag{7}$$

where the dummy indices M, N, N' and N'' represent loop sizes, N_T is the size of the chain, A denotes the rate of destruction of the loops of the corresponding size ($v_-(n)$,

which is the same for all N) and where $v_+(N_1; N_2)$ must be read as the rate of construction of the loops N_1 and N_2 simultaneously formed by closing an internal contact within a loop of size $N_1 + N_2 + 2$ already formed. The entropy change associated with such an event is $\Delta S = \Delta S(N_1) + \Delta S(N_2)$ and $p(N_1; N_2)$ is the probability of occurrence of such event.

Integration of equation (7) yields $P(N, t)$ which can be separated in five contributions whose relative importance is hereby assessed:

$$P(N, t) = P_0(N, t) + P_1(N, t) + P_2(N, t) + P_3(N, t) + P_4(N, t). \tag{8}$$

$P_0(N, t)$ is identical to $p(N, t)$ as it is the contribution to the total probability of the folding events which involve the closure of single loops without cooperative effects. $P_1(N, t)$ is the contribution of events which involve the formation of an interaction of range N already containing a loop of size N' (so the loop to close is of size $N - N' - 2$). $P_2(N, t)$ deals with interactions with two loops (of size N' and N'') already contained. $P_3(N, t)$ is yielded by the formation of interactions of range N inside a greater loop of size M already closed. $P_4(N, t)$ is similar to $P_3(N, t)$ but with another loop of size N' already formed inside the more external one.

Other kinds of cooperative folding events yield a negligible contribution, as our calculations reveal. $P_4(N, t)$ itself is negligible and $P_3(N, t)$ is only significant in the case of an external loop of critical size or smaller. In this case, the creation rate of the small interior loop would be big, since all polar groups would already be oriented pointing to the outer domain. In any case, for small loops $P_0(N, t) = p(N, t)$ is very big and $P_3(N, t)$ does not contribute to any appreciable extent to the total probability.

4. Results: the onset of cooperativity

Since folding events can be drastically affected by cooperative effects, the elucidation of kinetic folding pathways cannot be performed without a precise account of cooperativity. This means that we require a quantitative measure of cooperativity: we must not only evaluate its contribution to interactions of any range but also the time evolution of this contribution. This is the aim of the present section.

From equation (8), cooperativity (visualized in terms of $P(N, t)$–$p(N, t)$) can be quantified for any size of interaction. As revealed by figure 3, these cooperative effects are important for certain interactions near the critical loop size and they also produce an increase in the probability of occurrence of long-range interactions. These effects can bring the mean time of occurrence of some of these interactions within the otherwise too short biologically relevant (nonergodic) timescales.

The fact that cooperativity varies with time can be learnt from simple inspection of figure 3 where we display, with full curves, the profiles of $P(N, t)$–N at different times. There, we can see that cooperative effects are negligible at short timescales as the profile of $P(N, t)$–N (full curve) is practically the same as the one for $p(N, t)$–N (dotted curve) at the same time. However, at approximately $t = 5 \times 10^{-3}$ s the profile begins to change in a significant fashion, making apparent the onset of the cooperative effects. Then, the profile quickly acquires the shape that is maintained as t tends to infinity, that is, as the thermodynamic or ergodic regime is reached.

The first cooperative effects to appear in folding are what we can call cooperative effects of first order. They involve the existence of a first set of independent events and a second set of events dependent on the previous ones and, at the same time, independent of each other. The probability of occurrence of an overall event is the product of the probabilities

of occurrence of the two steps involved. For example, the two-step event which involves the closure of a loop already containing a previously formed loop is a cooperative event of first order. The probability $P^1(t)$ of occurrence of a specific kind of cooperative event of first order is given by

$$P^1(t) = (c/A^2)(1 - \exp[-At])^2 \tag{9}$$

where A is the rate of destruction of a loop (a constant for any loop size) and c contains the product of the rates of formation of the two steps involved. An example of a generic curve of $P^1(t)$ can be seen in figure 4. We can see that these curves (irrespective of the cooperative event of first order considered) present an inflection point in $\tau = \ln 2/A - 5.81$ ms. At this point in time all the $P^1(t)$ reach one fourth of their thermodynamic values and all the $p(N, t)$ reach one half of their corresponding thermodynamic values. This inflection point in the cooperativity contribution marks the site of departure of the $P(N, t)$–N profile from the $p(N, t)$–N profile, making apparent the onset of cooperativity, as we have seen before.

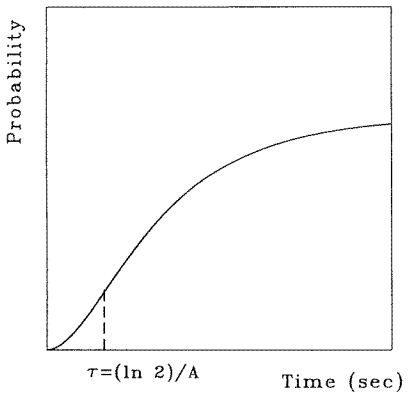

Figure 4. An example of the time evolution of the probability of occurrence of a cooperative event of the first kind ($P^1(t)$).

Cooperative events of higher order, involving more than two steps, present a lower probability of occurrence and appear later.

5. Inferences on dynamical folding pathways: the universal intermediate state

This section is devoted to the characterization of a universal folding intermediate whose existence can be inferred from inspection of the results expounded in the previous section. To postulate the existence of an intermediate is tantamount to assuming that there are two distinctive groups of events in the folding process. This is *precisely* what we have observed in section 4: initially, folding encompasses simple independent folding events which are subsequently followed by cooperative events.

Regardless of the compelling results of section 4 in what pertains to the existence of the universal kinetic intermediate, a rigorous justification for its existence will be developed in section 6. Section 6 is exclusively devoted to studying the averaged time-dependent behaviour of the Shannon information content of the conformation which is associated to the folding process. Thus, the time-dependent plot of Shannon's entropy presents a plateau in the range 10 ms–1 s. This feature occurs in both the folding of random heteropolymers

as well as in the folding of all 87 catalytically competent RNAs of the so-called group I intron family [18], thus furnishing overwhelming evidence in support of the existence of a kinetic intermediate. Beyond this level of folding, the Shannon entropy *monotonically* approaches its absolute minimum (zero).

The existence of the intermediate is a consequence of the exponential dependence of the unimolecular folding step timescales on the barrier size: a whole spectrum of interaction ranges, involving all events whose mean time of formation falls within the timespan of the folding process (of the order of seconds) can only be realized by means of cooperativity. Certain interactions cannot be formed independently since in the absence of cooperativity their associated timescales would be far longer than the total time allotted to the folding process. The onset of cooperativity as the only plausible expedient to realizing such interactions marks the endpoint in the lifetime of the kinetic intermediate.

This characterization of the first stages of the folding process involving secondary structure formation seems to be in accord with the experimental context.

Little is known on an experimental basis about the kinetics of folding of large RNAs. A key feature of group I introns that enables us to test the theory as resolved at secondary structure level is the fact that there is experimental [21–23] evidence that secondary structure formation precedes the formation of tertiary interactions.

A recent experimental study of the kinetics of folding of the Tetrahymena ribozyme RNA [7] supports the existence of a first kinetic intermediate characterized by secondary structure interactions readily formed even in the absence of Mg(II) ions. These fast interactions were found not to be essentially affected by the presence of Mg(II) ions. Further steps of the folding mechanism proposed involve high-order cooperativity and the latter ones imply tertiary structure formation. Some of these folding steps were found to require the presence of Mg(II) ions.

The first fast-occurring interactions may be due to the simple non-cooperative interactions which occur before $\tau = \ln 2/A \sim 5.81$ ms characterizing the first intermediate state, as shown in section 4. These interactions are either moderately long-range interactions or short-range ones. The moderately long-range interactions would not be affected by magnesium since they involve the closure of moderately big loops with no orientational entropy change involved. In turn, short-range interactions, which may be accelerated by the presence of Mg(II) ions by reducing the orientational entropy cost they involve, are themselves so fast that the effect of magnesium is not important. However, the steps that follow thereafter for the folding of the Tetrahymena ribozyme require high cooperativity. Recent theoretical work [24] expounded in section 6, rooted in the main ideas we have described here and taking into account the role of magnesium in lowering the kinetic barriers has shown that secondary structure formation is completed within approximately 100 s, in good agreement with the time experimentally observed [7]. Since the study we present here does not account for the effect of magnesium and is not concerned with tertiary structure motifs, we can only account for the first stages of the folding process. Further work in the way anticipated in section 2 will be required to fully place our study within the experimental context.

Similar findings regarding the possible universality of a kinetic intermediate have been suggested in the protein folding context by an increasing amount of experimental evidence (for reviews see Creighton [25] and Ptitsyn [26]). The key features of protein folding relevant to this issue are:

- The initial population of molecules in a refolding experiment is usually heterogeneous (the molecules are not all random coils but some differ slightly from a random coil). In any case, the final state is independent of the initial conditions [25].

• At the beginning of the folding process, each molecule follows a different folding pathway, but these pathways converge at certain point [25].

• Folding is a cooperative transition of first order. It is an all-or-none process: at the equilibrium, we have completely folded molecules or completely unfolded ones, without any appreciable population of molecules with an intermediate degree of folding [27].

• Folding is governed by only one rate-limiting step. All previous steps are faster. The molecules converge to a limited number of very similar conformations quickly and reversibly, attaining a pre-equilibrium in an intermediate state [28–35].

• The intermediate state occurs late in the folding process, that is, it is structurally very similar to the final state, with the major amount of the secondary structure already formed [29].

• In refolding experiments, the majority of the secondary structure is restored within 0.01 s and secondary structure formation precedes the formation of tertiary structure [34, 36–39].

These results suggest an emerging general picture in which a universal kinetic intermediate is formed. However, the protein folding context lies outside the scope of this work.

The intermediate conformation in RNA folding is independent of the initial conditions since, in its initial stages, the cooperative effects are negligible and all the molecules tend to form all the simple loops dictated by the profile $p(N,t)$–N until they saturate this possibility. Obviously, the final structure thus resulting is independent of the choice of initial conditions.

Although each molecule follows a different pathway, all form in an appreciable extent the same contacts and converge accumulating in an intermediate state practically identical. This fact is responsible for a drastic reduction in the number of possibilities for further relaxation and, thus, of the final destination of the folding process. As it has been said before, the life of the intermediate comes to an end once the onset of cooperativity takes place. This universal point was found to be $\tau = \ln 2/A \sim 5.81$ ms, as shown in section 4. The ranges of interactions which characterize the intermediate state are those which involve the closure of simple loops with a mean time of formation compatible with τ. These are the interactions within the ranges $N = 3$ to $N = 6$ and $N = 18$ to $N = 108$ (with N in real units, that is, the number of unpaired nucleotides in the loop). Since τ represents an inflection point in the cooperative effects of first order, the cooperative events cannot be completely neglected for shorter timescales. Nevertheless, for $t < \tau$, the cooperative events are less probable than the least probable simple events which characterize the intermediate state. This can be seen in figure 5 where we compare the probability of occurrence of a single loop of size $N = 108$, the least probable simple loop with mean time of formation compatible with the intermediate lifetime, with one of the cooperative events with the higher probability (a cooperative event of first order involving the closure of two tetraloops). This fact rules out the possibility of occurrence of a 'cascade of events', that is, cooperative events of high order involving the closure of very stable loops at each step.

Once the life of the intermediate has come to an end, the molecules can complete their folding, forming the less favourable interactions, via the cooperativity expedient and establishing tertiary interactions. The fact that the intermediate state is similar to the final state can be explained since the majority of the native contacts which involve the closure of simple independent loops minimizing the contribution $-T\Delta S_{loop}$ are formed before the profile of $P(N,t)$ versus N begins to change, that is, before the appearance of cooperativity.

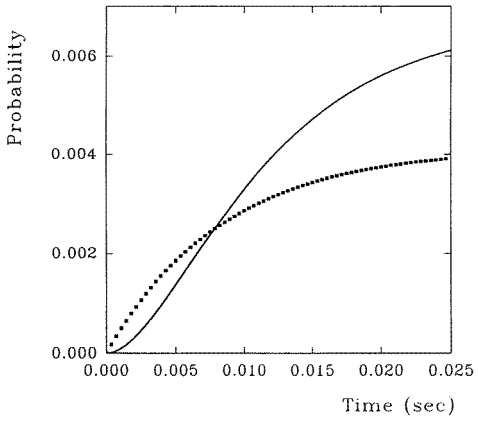

Figure 5. Comparison of the time dependence of the probability of occurrence of the independent simple event of closing a loop of size 108 (dotted curve) with the first-order cooperative event involving the closure of two tetraloops (solid curve). Loop sizes are given in real units.

6. The universal intermediate state as revealed by the time-dependent information content

A rigorous justification for the existence of a universal kinetic intermediate demands that we prove a prevailing and temporary stagnation in the growth of information content concurrent with the folding process. Thus, a time-dependent plot of Shannon's entropy should display a plateau within the 10 ms–1 s range in accord with the findings of sections 4 and 5.

To be precise, we shall start by specifying the degree of coarse graining of conformation space X. In our coarse description two RNA conformations are regarded as equivalent if they share the same BPP. This equivalence relation determines a partition Z of X in mutually disjoint equivalence classes.

Given the partition Z and a stochastic process ξ defining transition probabilities between elements of Z at each given time, we may define a coarse dynamical system entropy $\sigma(t)$ associated to the partition Z in the following way:

$$\sigma(t) = -\sum_{A\in Z} \pi_t\eta(A)\ln[\pi_t\eta(A)] \tag{10}$$

where A is a generic BPP, η is the probability measure in the space Θ of folding pathways $\vartheta's(\vartheta \in \Theta)$ determined by our stochastic process [40, 41], and $\pi_t\eta$ is the projection of measure η at the instant t. This projection actually yields the weight distribution among BPPs at time t and can be easily computed using our folding algorithm [3, 16, 42, 43]

$$\pi_t\eta(A) = \eta\{\vartheta \in \Theta; \pi_t\vartheta = \vartheta(t) \in A\} = \Omega(A,t)/\Omega \tag{11}$$

where $\Omega(A,t)$ is the number of generated folding pathways passing through A at time t and Ω is the total number of generated folding pathways.

Direct inspection of equation (10) shows that our coarse entropy $\sigma(t)$ is minus a Shannon information content, since $\pi_t\eta(A)$ may be interpreted as the probability of finding a single molecule folded in BPP A at time t.

In order to determine the behaviour of $\sigma(t)$ during the folding of specific RNA molecules, we first specify the process ξ. To implement the process at the computational level, we first make use of current combinatorial algorithms (see, for example, [44]) to predict all plausible BPPs. Such algorithms incorporate the pseudoknot as a tertiary

interaction motif and consider only base pairing and stacking as stabilizing interactions in intramolecular structure.

The stochastic process is determined by the activation energy barriers required to produce or dismantle stabilizing interactions. Thus, at each instant, the partially folded chain undergoes a series of disjoint elementary events with transition probabilities dictated by the unimolecular rates of the events. The stochastic process is Markovian since the choice of the set of disjoint events at each stage of folding is independent of the history that led to that particular stage of the process [3, 16, 42, 43]. The process is mechanistically constructed as follows. For each time $t \in I$, we define a map $t \to J(x,t) = \{j : 1 \leqslant j \leqslant n(x,t)\}$, where $J(x,t)$ is the collection of *elementary* events representing conformational changes which are feasible at time t given that the initial conformation x has been chosen at time $t = 0$, and $n(x,t)$ is the number of possible elementary events at time t. Associated to each event there is a unimolecular rate constant $k_j(x,t)$, the rate constant for the jth event [16, 42] which may take place at time t for a process that starts with conformation x. The mean time for an elementary refolding event is the reciprocal of its unimolecular rate constant. Thus, for a fixed time interval I, the only elementary events allowed are elementary refolding events that satisfy $k_j(x,t)^{-1} \leqslant |I|$. We now introduce a random variable $r \in [0, \sum_{j=1}^{n(x,t)} k_j(x,t)]$, uniformly distributed over the interval. Let r^* be a particular realization of r arising in a simulation of the process. Then there exists an index j^* such that

$$\sum_{j=0}^{j^*-1} k_j(x,t) < r^* \leqslant \sum_{j=0}^{j^*} k_j(x,t), \qquad (k_0(x,t) = 0 \text{ for any } x,t). \tag{12}$$

This implies that the event $j^* = j^*(x,t)$ is chosen at time t for the folding process that starts at conformation x. Thus, the map $t \to j^*(x,t)$ for fixed initial condition x constitutes a realization of the Markov process which determines the folding pathway ξ_x. In turn, the probability that the j^*-event is chosen at time t is

$$\left(k_{j^*}(x,t) \Big/ \sum_{j' \in J(x,t)} k_{j'}(x,t) \right).$$

Explicit values of the unimolecular rate constants require an updated compilation of the thermodynamic parameters at renaturation conditions [45]. These parameters are used to generate the set of kinetic barriers associated to the formation and dismantling of stabilizing interactions, the elementary events in our context of interest. The rate constants k_js are precisely those displayed in equation (4), except that the number of base-pairing contacts, n, is not fixed because we are treating both random as well as *real sequences*. In the latter case $n \geqslant 3$.

At this point we can present computations of the coarse entropy $\sigma(t)$ for specific RNA sequences in order to verify the existence of the universal kinetic intermediate. The behaviour was determined by monitoring σ concurrently with the running of Monte Carlo simulations making use of working equations (10)–(12) and (4). Taking into account the working equations and the mechanistic generation of folding pathways, the number of MC steps can be effectively correlated with real time: $10^6 = 100$ s, $10^5 = 1$ s, $10^4 = 10$ ms, $10^3 = 100$ μs, $10^2 = 1$ μs. The folding of all 87 catalytic RNAs (ribozymes) of the so-called group I intron family [46, 47] was examined using the compilation of thermodynamic parameters [45] specified by the renaturation conditions of the experiments presented in [7]. A drastic reduction of the coarse entropy (slightly higher than 50%) takes place within the 10 ms timescale. This reduction corresponds to the simultaneous occurrence of disjoint noncooperative folding events leading to stabilizing interactions with low or moderately low kinetic barriers. Such interactions cover the ranges $4 \leqslant N \leqslant 14$ and

$24 \leqslant N \leqslant 100$. The plateau reached after completion of 10^4 MC steps (10 ms) corresponds to a kinetic intermediate which is experimentally identifiable: it contains all noncooperative phylogenetically conserved interactions excluding the pseudoknot motif [7]. The second major and decisive reduction of coarse entropy leads to its absolute minimum *only* for the biological sequences. It is achieved in the 100 s timescale (10^6 MC steps) and corresponds to the occurrence of cooperative events. Such events result in the formation of interactions of an unfavourable range when viewed starting from the random coil. These interactions require closure of pseudoknotted and complex internal loops which, in turn, require the prior occurrence of nucleating interactions of favourable ranges. The net effect of such nucleating interactions is the shortening of the length of loops for the initially unfavourable interactions. Nucleating interactions have already occurred in the 10 ms timescale and determine a predictable and detectable [7, 47] kinetic folding intermediate.

For the sake of illustration, the results are displayed in figure 6 for two selected ribozymes of the group I family. Standard notation has been adopted and the primary

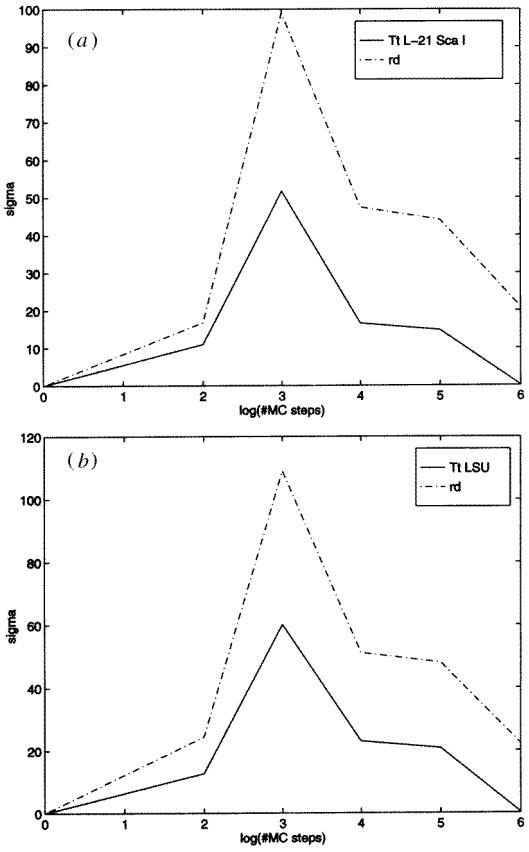

Figure 6. Time-dependent behaviour of the coarse entropy σ for two specific ribozymes of group I. The abscissas correspond to the logarithm of the number of Monte Carlo (MC) steps performed in the simulations. (*a*) The full curve corresponds to the species TtL–21 ScaI and the broken curve corresponds to a random sequence of the same length (404 nucleotides). (*b*) Full curve for the species TtLSU and broken curve for its random counterpart (length = 414 nucleotides).

sequences have been obtained from [46]. In order to assess their folding efficiency, a comparison with random sequences (rd) of the same length was included in figure 6.

7. Concluding remarks

We have derived a general picture of the chronology of occurrence of interactions of different ranges in biopolymer folding. The results are specialized for RNA folding subject to severe time constraints. The distribution of destination structures for such a process cannot in general be equated with the Boltzmann distribution. Our results rooted in a rigorous treatment of the kinetics of the folding process reveal an initial accumulation of the molecules in an intermediate state with the concurrent drastic reduction in the number of possibilities for future folding events. This picture accounts for the short timescales involved in the restoration of the majority of the secondary native structure found in protein and RNA refolding and renaturation experiments [7, 34, 36–39], and explains the robustness and expediency of the folding process, bypassing Levinthal's scenario [1].

Acknowledgments

AF is principal investigator of CONICET, the National Research Council of Argentina. This work was performed during the tenure of a JS Guggenheim Memorial Foundation Fellowship awarded to AF. Helpful discussions with Professor Herschal Rabitz are gratefully acknowledged.

References

[1] Levinthal C 1969 *Mössbauer Spectroscopy in Biological Systems* ed P Debrunner *et al* (Urbana, IL: University of Illinois Press) pp 22–4
[2] Fernández A 1990 *Phys. Rev. Lett.* **65** 2259
[3] Fernández A 1992 *Phys. Rev.* A **45** R8348
[4] Fernández A and Shakhnovich E I 1990 *Phys. Rev.* A **42** R3657
[5] Frauenfelder H, Sligar S G and Wolynes P 1991 *Science* **254** 1598
[6] Fernández A, Arias H and Guerín D 1995 *Phys. Rev.* E **52** R1299
[7] Zarrinkar P P and Williamson J R 1994 *Science* **265** 918
[8] Pleij C W, Rietveld K and Bosch L 1985 *Nucleic Acids Res.* **13** 1717
[9] Tanford C 1962 *J. Am. Chem. Soc.* **84** 4240
[10] Pace N 1975 *CRC Crit. Rev. Biochem.*
[11] Privalov P L and Kechinashvilli N N 1974 *J. Mol. Biol.* **86** 665
[12] Privalov P L 1979 *Adv. Protein Chem.* **33** 167
[13] Dill K A 1985 *Biochemistry* **24** 1501
[14] Dill K A 1988 Conformational entropy and protein stability *Protein Structure and Protein Engineering* ed E L Winnacker and R Huber (Berlin: Springer)
[15] Privalov P L 1988 Hydrophobic interactions in proteins *Protein Structure and Protein Engineering* ed E L Winnacker and R Huber (Berlin: Springer)
[16] Fernández A 1990 *Phys. Rev. Lett.* **64** 2328
[17] Anshelevich V V, Vologodskii V A, Lukashin A V and Frank-Kamenetskii M D 1984 *Biopolymers* **23** 39
[18] Fernández A, Appignanesi G and Cendra H 1995 *Chem. Phys. Lett.* **262** 460
[19] Cantor C and Schimmel P R 1980 *Biophysical Chemistry* vol III (San Francisco, CA: Freeman)
[20] Pan T, Long D and Uhlenbeck O C 1993 *The RNA world* ed R F Gesteland and J F Atkins (New York: Cold Spring Harbor Laboratory Press) ch 12, pp 221–302
[21] Crothers D M, Cole P E, Hilbers C W and Shulman R G 1974 *J. Mol. Biol.* **87** 63
[22] Banerjee A R, Jaeger J A and Turner D H 1993 *Biochemistry* **32** 153
[23] Jaeger L, Westhof E and Michel T 1993 *J. Mol. Biol.* **234** 331

[24] Fernández A 1996 The expediency of RNA folding as revealed by the maximization in information content *Physica* **A** in press
[25] Creighton T E 1990 Understanding protein folding pathways and mechanisms *Protein Folding* ed L M Gierasch and J King (Washington, DC: American Association for the Advancement of Science) p 157
[26] Ptitsyn O B and Semisotnov G V 1991 The mechanism of protein folding *Conformations and Forces in Protein Folding* ed B T Nall and K A Dill (Washington, DC: American Association for the Advancement of Science) p 155
[27] Privalov P L 1979 *Adv. Protein Chem.* **33** 167
[28] Kuwajima K J 1977 *J. Mol. Biol.* **114** 241
[29] Creighton T E 1980 *J. Mol. Biol.* **137** 61
[30] Kato S, Okamura M, Shimamoto N and Utiyama H 1981 *Biochemistry* **20** 1080
[31] Denton J B, Konishi Y and Scheraga H A 1982 *Biochemistry* **21** 5155
[32] Lynn R M, Konishi Y and Scheraga H A 1984 *Biochemistry* **23** 2470
[33] Ikeguchi M, Kuwajima K, Mitani M and Sugai S 1986 *Biochemistry* **25** 6965
[34] Kuwajima K J, Yamaya H, Miwa S, Sugai S and Magamura T 1987 *FEBS Lett.* **221** 115
[35] Ptitsyn O B 1987 *J. Protein Chem.* **6** 273
[36] Gilmanshin R J and Ptitsyn O B 1987 *FEBS Lett.* **223** 327
[37] Gilmanshin R J, Ptitsyn O B and Semisotnov G V 1988 *Biofizika (USSR)* **33** 204
[38] Kuwajima K J, Sakuruaka A, Fueki S, Yoneyama M and Sugai S 1988 *Biochemistry* **27** 7419
[39] Goldberg M E, Semisotnov G V, Friguet B, Kuwagima K J, Ptitsyn O B and Sugai S 1990 *FEBS Lett.* **263** 51
[40] Kakutani S 1943 *Proc. Imp. Acad. Japan* **29** 184
[41] Fernández A 1994 *J. Stat. Phys.* **77** 1079
[42] Fernández A 1989 *Eur. J. Biochem.* **182** 161
[43] Fernández A 1993 *Physica* **201A** 557
[44] Gautheret D, Major F and Cedergren R 1989 *Methods in Enzymology* **183** 318
[45] Jaeger J A, Turner D H and Zucker M 1989 *Proc. Natl Acad. Sci., USA* **86** 7706
[46] Michel F and Westhof E 1990 *J. Mol. Biol.* **216** 585
[47] Gesteland R F and Atkins J F ed 1993 *The RNA World* (New York: Cold Spring Harbor Laboratory Press)